The Journal of Nutritional Biochemistry
Volume 107, September 2022, 109056

Research Paper

Nicotinamide reprograms adipose cellular metabolism and increases mitochondrial biogenesis to ameliorate obesity

Chengting Luo [a, b], Changmei Yang [b], Xueying Wang [c], Yuling Chen [a, b], Xiaohui Liu [c] ✉, Haiteng Deng [a, b, c] ✉

[a] Tsinghua-Peking Center for Life Sciences, Tsinghua University, Beijing, China
[b] MOE Key Laboratory of Bioinformatics, Center for Synthetic and Systematic Biology, School of Life Sciences, Tsinghua University, Beijing, China
[c] Technology Center of Protein Research, Tsinghua University, Beijing, China

Received 6 September 2021, Revised 22 March 2022, Accepted 6 April 2022, Available online 21 May 2022, Version of Record 15 June 2022.

https://doi.org/10.1016/j.jnutbio.2022.109056

Abstract

Obesity poses a global health challenge and is a major risk factor for diabetes mellitus, cardiovascular diseases, hypertension, stroke and certain kinds of cancers. Although the effects of nicotinamide (NAM) on liver metabolism and diseases were well documented, its effects on adipose tissue are yet to be characterized. Herein, we found that NAM supplementation

significantly reduced fat mass and improved glucose tolerance in obese mice. Proteomic analysis revealed that NAM supplementation upregulates mitochondrial proteins while quantitative polymerase chain reaction showed that PPARα and PGC1α were both upregulated in adipose tissues, proposing that NAM increased mitochondrial biogenesis in adipose tissue. Indeed, NAM treatment increased proteins related to mitochondrial functions including oxidative phosphorylation, fatty acid oxidation, and TCA cycle. Furthermore, isotope-tracing assisted metabolic profiling revealed that NAM activated NAMPT and increased cellular NAD^+ level by 30%. Unexpectedly, we found that NAM also increased glucose derived amino acids to enhance glutathione synthesis for maintaining cellular redox homeostasis. Taken together, our results demonstrated that NAM reprogramed cellular metabolism, enhanced adipose mitochondrial functions to ameliorate symptoms associated with obesity.

Previous Next

Key words

Nicotinamide; Obesity; Nicotinamide adenine dinucleotide (NAD+); Glutathione; Mitochondrial biogenesis

1. Introduction

Obesity and associated diseases, such as stroke, cardiovascular diseases, diabetes, and certain cancers are becoming global epidemic. According to the ageing and health fact sheet from World Health Organization, over two billion people worldwide are overweight and nearly 35% of these individuals are severely obese [1]. Nicotinamide adenine dinucleotide (NAD^+), one of the biological redox cofactors, plays a central role in cellular energy regulation and metabolism. NAD^+ has gained a resurgence of interest over recent years for its roles in obesity. It has been documented that NAD^+ levels decrease in adipose tissue, liver, and muscle of obese rodents and human [2], [3], [4], [5]. Furthermore, interventions such as exercise and calorie restriction ameliorate metabolic disorders by increasing NAD^+ content [6], [7], [8], [9].

Nicotinic acid, nicotinamide (NAM), nicotinamide riboside, and nicotinamide mononucleotide (NMN) are NAD^+ precursors. Metabolic flux analysis in mice showed that NAD^+ synthesis in adipose tissue, muscle, and brain relied on circulating NAM, postulating the crucial role of NAM [10,11]. It was reported that NAM supplementation improved insulin sensitivity in diabetic human and rodent models [12], [13], [14]. NAM also decreased oxidative stress and protected hepatocytes against saturated fatty acids-induced cell death in obese rats [14], [15], [16]. Recently, Mitchell et al. used a high dose NAM to treat aged mice and found that NAM prevented

hepatosteatosis and ameliorated liver glucose metabolism by inhibiting de novo lipid synthesis [17,18]. NAM increased lipid catabolism by upregulating genes associated with carnitine synthesis in obese rat liver and muscle [19]. Molecular mechanisms of NAM were deeply investigated in liver tissue, but the effects of NAM on adipose tissue have not been comprehensively investigated.

In the present work, we aimed to examine the effects of NAM on the fat loss and lipid metabolism in obese mice induced by a high fat diet. We performed multi-omics analysis including quantitative proteomics, metabolomics, lipidomics, and isotope tracing analysis to delineate the effects of NAM supplementation on adipose tissue. We reveal that NAM supplementation reverse obesity and ameliorate comorbidities associated with obesity by boosting NAD^+, enhancing oxidation of fatty acids and increasing GSH biosynthesis.

2. Materials and methods

2.1. Animal experiments

Mice experiments were performed in the animal facility of Tsinghua University (Beijing, China) with approval of the Institutional Animal Care and Use Committee of Tsinghua University. C57BL/6J WT mice was purchased from Jackson Laboratory through Laboratory Animal Research Center and housed in animal facility of Tsinghua University with ad libitum access to diet and tap water. Animal rooms were maintained at 20–22°C with 30–70% relative humidity and a 12-h light/dark cycle. Four-week C57BL/6J male mice were fed high fat diet (Research Diets, New Brunswick, USA, D12492, with 60 kcal% fat) for 8 weeks, and then randomized into two groups: one fed normal water and the other fed water with NAM (Sigma-Aldrich, N0636) supplementation (18.75 g NAM/100 mL water as a clear solution) which was corresponding with 37.5 mg/g BW/d [17]. Mice were continuously fed a high-fat diet throughout the study. Bodyweight and food intake were examined every 1 week from NAM supplementation to the sacrifice of mice. Metabolic cage (TSE, Germany, 30202-c-08) and glucose tolerance test were performed during the third week of NAM supplementation. Animals were sacrificed at the end of third week, and liver, brown adipose tissue (BAT), subcutaneous adipose tissue (SCAT), and epididymal adipose tissue (eWAT) were weighed, frozen quickly in liquid nitrogen and stored at –80°C. Blood protein aspartate aminotransferase (AST), lactate dehydrogenase (LDH), creatine kinase (CK), and alkaline phosphatase (ALP) were measured with Roche Cobas 6000 (C501) Chemistry Analyzer.

2.2. Cell cultures

3T3L1 pre-adipocytes cells were purchased from American Type Culture Collection and were grown in Dulbecco's Modified Eagle's Medium (DMEM) (Wisent, Nanjing, China) supplemented with 10% fetal bovine serum (FBS), 100 U/mL penicillin, and 100 μg/mL streptomycin (Wisent, Nanjing, China) in a humidified incubator containing 5% CO_2 at 37°C. 3T3-L1 pre-adipocytes were induced to differentiated mature adipocytes as described by the protocol of American Type

Culture Collection. In brief, cells were grown 2 d after confluence in DMEM/FBS and then in DMEM/FBS supplemented with 5 μg/mL insulin, 1 μM dexamethasone, and 0.5 mM isobutylmethylxanthine for an additional 2 d. The medium was then changed to DMEM/FBS supplemented with 5 μg/mL insulin. Cells were used for experiments 8 d after differentiation.

2.3. Quantitative proteomic analysis by LC-MS/MS

Proteomic analysis was carried out as described previously [20]. Firstly, about 100 mg subcutaneous adipose tissue was homogenized with radioimmunoprecipitation assay buffer, centrifuge at 4°C to collect the supernatant. Then mix the supernatant with iced acetone as one volume supernatant: four volume acetone for 4 h at –20°C to precipitate protein. Dissolved the precipitate with 8 M urea and then 100 μg protein from each sample was digested with trypsin for 16 h at 37°C. Next, tryptic peptides were desalted and labeled with the tandem mass tag (TMT, Thermo Fisher Scientific, Waltham, MA, USA, 90061), according to the manufacturer's protocol. The labelled peptides then were mixed, desalted and separated by reverse phase chromatography. Lastly, MS data was acquired with data-dependent acquisition method by Orbitrap Q-Exactive mass spectrometer, utilizing Xcalibur 3.0 software (Thermo Fisher Scientific, Waltham, MA, USA). The MS/MS spectra from the mass spectrometer were searched across the UniProt mice database using the SEQUEST search engine of Proteome Discoverer software (version 2.1).

2.4. Metabolome analysis

Iced methanol extraction was used to collect of tissue metabolites as previously established [21]. Briefly, about 100 mg subcutaneous adipose tissue was homogenized with pre-chilled 80% methanol (–80°C). Then, macromolecules and debris were removed by centrifugation at 14,000 g for 20 min at 4°C. The metabolites within the supernatant were concentrated by drying completely using a Speedvac (Labconco, Kansas City, USA) for mass spectroscopy analysis. The chromatographic peak area was used to quantitated the relative abundance of a metabolite.

2.5. Isotope tracing metabolomics

The isotope tracing metabolomics was carried out following a method we reported previously [22]. For NAD^+ tracing experiment, related to Fig. 2, we cultured 3T3L1 cells using glucose-free DMEM, supplemented with 4.5 g/L $^{13}C_6$-glucose (Cambridge Isotope Laboratories, Andover, MA, USA, CLM-1396) for 24 h. For glutathione tracing experiments, related to Fig. 4, we cultured 3T3L1 cells using glucose and glutamine-free DMEM supplemented with 4.5 g/L $^{13}C_6$-glucose for 24 h. In parallel with this, an unlabeled culture was prepared by adding equal concentrations of unlabeled glucose to the medium to identify endogenous metabolites. The metabolites were extracted by cold methanol extraction methods for LC-MS/MS analysis. Detecting metabolites in tracing experiments used The Dionex Ultimate 3000 UPLC system coupled to a TSQ Quantiva Ultra triple-quadrupole mass spectrometer (Thermo Fisher Scientific, Waltham, MA, USA), equipped with a heated electrospray ionization probe. Extracts were separated by a synergi

Hydro-reverse phase column (2.0 × 100 mm, 2.5 μm, phenomenex). A binary solvent system was used, in which mobile phase A consisted of 10 mM tributylamine adjusted with 15 mM acetic acid in water, and mobile phase B of methanol. This analysis used a 25-min gradient from 5% to 90% mobile B. Data acquired in selected reaction monitoring for metabolites in positive-negative ion switching mode. The resolution for Q1 and Q3 are both 0.7 FWHM. The source voltage was set at 3500 v for positive- or 2500 v for negative-ion mode. The source parameters are set as follows: capillary temperature: 350°C; heater temperature: 300°C; sheath gas flow rate: 35; auxiliary gas flow rate: 10. Tracefinder 3.2 (Thermo Fisher Scientific, Waltham, MA, USA) was applied for metabolite identification and peak integration.

2.6. Ingenuity pathway analysis

Significantly changed proteins (fold change < 0.76 or >1.30, $P < .05$) were uploaded to Ingenuity Pathway Analysis software to perform pathway analysis. The pathways' *P*-values were calculated based on Fisher's exact test right-tailed methods. The match between observed gene expression and expected relationship direction is presented as z-score. Z-score >2 is considered that pathway is significantly activated, and z-score < –2 is considered that pathway is significantly inhibited [23].

2.7. Immunoprecipitation and Western Blot

The total protein was extracted from fat tissue and immunoprecipitation assay was performed using protein A/G beads (Thermo Fisher Scientific, Waltham, MA, USA, 78609). Briefly, equal amount of protein from each adipose homogenate was immunoprecipitated with protein A/G beads and SOD2 antibody (Cell Signaling Technology, Boston, MA, USA, 13141) rotated overnight at 4°C in a rotary wheel. Then, the beads were washed three times, boiled with loading buffer and separated on sodium dodecyl sulfate–polyacrylamide gel electrophoresis gel. For western blotting, cells lysates and tissue homogenate were prepared with radioimmunoprecipitation assay buffer at 4°C. Equal amount of protein was subjected to sodium dodecyl sulfate–polyacrylamide gel electrophoresis and then transferred onto a polyvinylidene difluoride membrane. After blocked with 5% skimmed milk, the membrane was incubated with first antibodies against NAMPT (Cell Signaling Technology, Boston, MA, USA, 61122), COXIV (Abcam, Waltham, MA, USA, AB33985), GDH1 (Proteintech, Rosemont, USA, 14299-1-AP), Acetylated lysine (Millipore, Millipore, Burlington, MA, USA, 2452518), or β-actin (Cell Signaling Technology, Boston, MA, USA, 3700) at 4°C overnight. HRP-conjugated secondary antibodies at room temperature for 1 h. The proteins on the membrane were detected by using enhanced chemiluminescence.

2.8. RNA extraction and real-time polymerase chain reaction

Total RNA was extracted from cells or adipose tissue using TRIzol extraction method. Complementary DNA was synthesized from 1 μg total RNA using reverse transcription system according to the manufacturer's protocols (CWbiotech, Beijing, China, CW0659). Quantitative

real-time polymerase chain reaction was performed with the Roche LightCycler 480II Detection System with SYBR green according to the manufacturer's instructions and the β-actin was used as an internal reference. Primers used in this study were listed in Table S2.

2.9. Glucose tolerance test

Glucose tolerance test was performed with a dose of 2 g glucose/ kg BW, intraperitoneally injected to 16-h fasted mice, and tail vein blood were collected at predefined time intervals (0, 15, 30, and 60) for blood glucose assessment.

2.10. Quantification and statistical analysis

Statistical analysis was performed using GraphPad Prism (version 7.0). Data were shown as mean ± SD. Independent samples between two groups used student t-test to analyze differences of mean values and the significance was established at $P < .05$.

2.11. Body composition analysis

Fat mass and lean mass were measured with EchoMRI analyzer (Houston, USA). Firstly, calibrate the system with a standard subject which was pure oil weighed of 30.3 g. The calibration need about 5 min and then place mice into container and begin to scan the composition of each mouse. Each mouse was scanned 3 times and the average value served as readout. During scanning, there was no need to anaesthetize the mouse and the duration of scanning one mouse was about 2 min.

2.12. Data and code availability

The mass spectrometry proteomics data have been deposited to the ProteomeXchange Consortium via the PRoteomics IDEntifications are available via ProteomeXchange with identifier PXD019089 [24].

3. Result

3.1. NAM effectively decreased fat accumulation in diet-induced-obesity mice

Previous studies indicated that long-term treatment with NAM induced glucose intolerance and skeletal muscle lipid accumulation [25,26], and thus we aimed to examine whether a short-term NAM treatment can ameliorate diet-induced-obesity (DIO). A 3-week NAM supplementation significantly decreased the body weight in mice (Fig. 1A). NAM also decreased fat mass by 47% as measured by magnetic resonance imaging (9.39 ± 0.64 g fat mass of CTR group *vs.* 2.94 ± 0.27 g of NAM group), while lean mass was increased by 1.4-fold (22.04 ± 0.46 g lean mass of CTR group *vs.* 18.55 ± 1.35 g of NAM group) (Fig. 1B). In addition, weights of SCAT, eWAT, BAT, and liver were all significantly decreased (Fig. 1C). Especially, the volume of SCAT and eWAT also declined

(Fig. 1D). Consistently, HE staining showed that NAM decreased hepatic lipid content and the size of adipocytes from several anatomical locations including SCAT, eWAT, and BAT (Fig. 1E). In addition, NAM supplementation lowered the glucose level at each time point over glucose tolerance test (GTT) (Fig. S1A and B). Meanwhile, we observed carefully raw phenotype of the mice treated with NAM, and no symptoms including diarrhoea and vomiting were observed during NAM supplementation. In addition, we found hair color of NAM-treated mice looked black and glossy as control group mice did with less oil on the surface of hair induced by high fat diet than control group (Fig. S1C). NAM-treated mice move as much as control group and showed similar day-night rhythm (Fig. S1D). Food intakes were similar between mice treated with NAM and control (Fig. S1E). In order to examine whether NAM supplementation induced injury of liver and heart, we checked the serum protein AST, LDH, and CK. We found that AST and CK were not changed (Fig. S1F and G), and LDH were decreased by NAM treatment (Fig. S1H), indicating NAM supplementation did not change significant injury of liver and heart. In addition, after measuring serum content of creatinine and uric acid by LC-MS/MS, we found that level of creatinine was not changed and uric acid even decreased (Fig. S1I and J), so it can be concluded that NAM supplementation did not lead to injury of kidney. Furthermore, we examined the effects of NAM on 16-week C57BL/6J male mice fed a chow diet. NAM decreased body weight of mice fed a normal diet (Fig. S1K). As obese mice, AST, ALP, CK, or LDH were not increased by NAM supplementation, suggesting NAM supplementation did not induce injury of liver and heart (Fig. S1L–O). The data indicated that NAM reduced fat content in DIO mice and improved glucose metabolism.

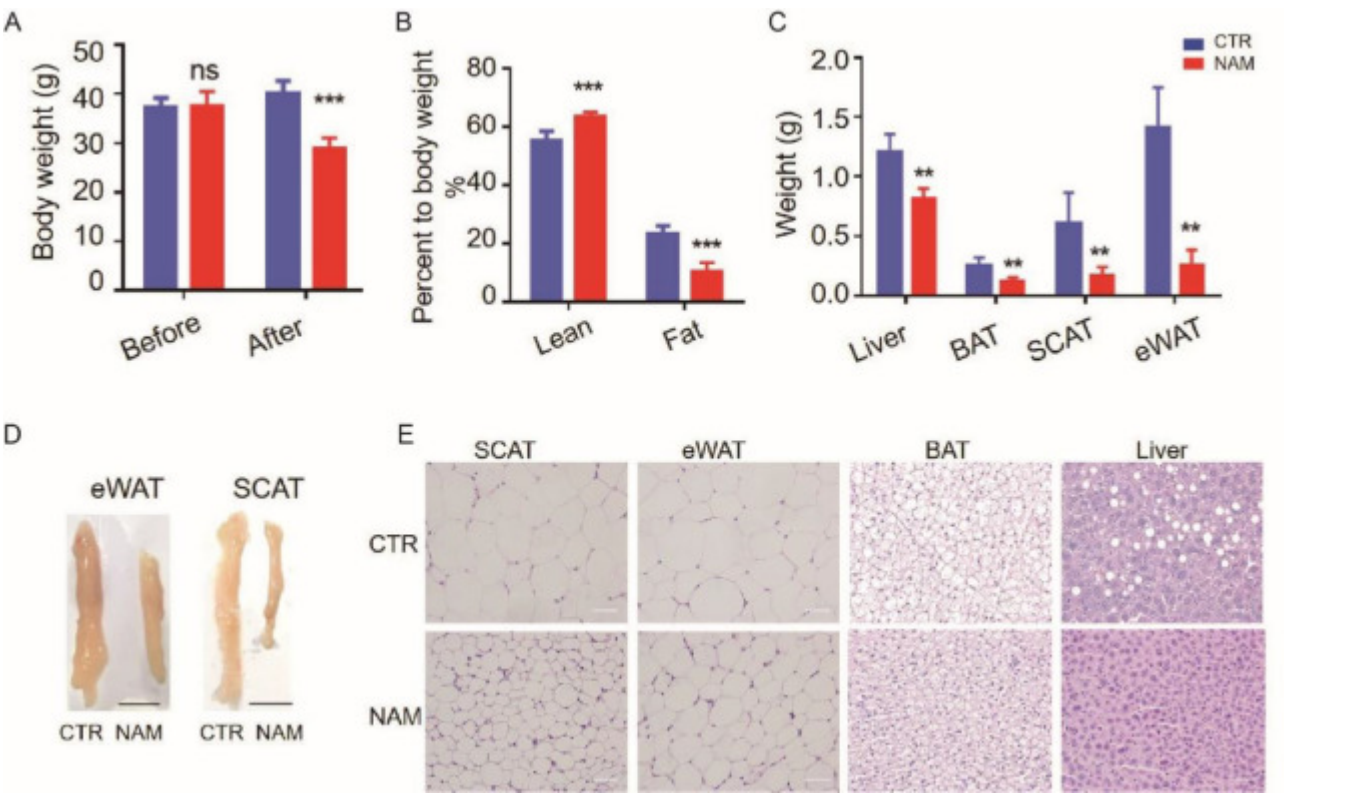

Download : Download high-res image (686KB) Download : Download full-size image

Fig. 1. NAM supplementation reduced fat accumulation. (A) NAM supplementation decreased bodyweight of high fat diet induced obese mice. Data were presented as mean ± SD. Statistical significance was calculated between NAM and control group mice, $^{***}P < .001$, $n = 6$ mice per group. (B) NAM supplementation decreased percentage of fat mass to body weight and increased percentage of lean mass to body weight. Data were presented as mean ± SD. $^{***}P < .001$, $n = 6$ mice per group. (C) Wet weight of liver, subcutaneous adipose tissue (SCAT), epididymal adipose tissue (eWAT), brown adipose tissue (BAT) of control and NAM treated mice. Data were presented as mean ± SD. $^{**}P < .01$, $n = 6$ mice per group. (D) Representative photograph of SCAT and eWAT dissected from mice under NAM supplementation or control, scale bar = 1 cm. (E) Representative HE staining of liver, BAT, SCAT, and eWAT, scale bar = 50 μm. HE, h ematoxylin and eosin; NAM, nicotinamide; ns, not significant.

3.2. NAM increased NAMPT to enhance NAD^+ biosynthesis

In order to examine the changes in NAM associated metabolites upon NAM supplementation in SCAT, we performed targeted metabolic analysis. As showed in Figure 2A, NAD^+, $NADP^+$, NAM, and N^1-methylnicotinamide were all dramatically increased in adipose tissue from NAM-treated mice. The total pool size of NAD^+ is dependent on the relative rates of synthesis and degradation, so we checked the level of NAMPT. Consistently with the increase in NAD^+ level, western blot analysis showed that NAMPT was increased about 1.6-fold (Fig. 2B and S2A). To further characterize the effects of NAM on cellular metabolism, we measured the levels of cellular NAD^+ at 1 mM and 5 mM, but NAD^+ level increased less than 1.5-fold even at concentration of 5 mM NAM (Fig. S2B). In order to boosted NAD^+ level, so we tried to use higher concentration of NAM (10 mM). Examined with oil red o staining, 10 mM NAM treatment did not change cell morphology or induce cell debris accumulation (Fig. S2C). So we performed isotope-tracing assisted metabolic profiling in 3T3L1 cells to examine the biosynthesis of NAD^+ from NAM at 10 mM. Briefly, 3T3L1 cells were cultured in DMEM supplemented with $^{13}C_6$-glucose instead of normal glucose upon NAM treatment and metabolites were analyzed with LC-MS/MS to identify metabolites containing ^{13}C atoms.

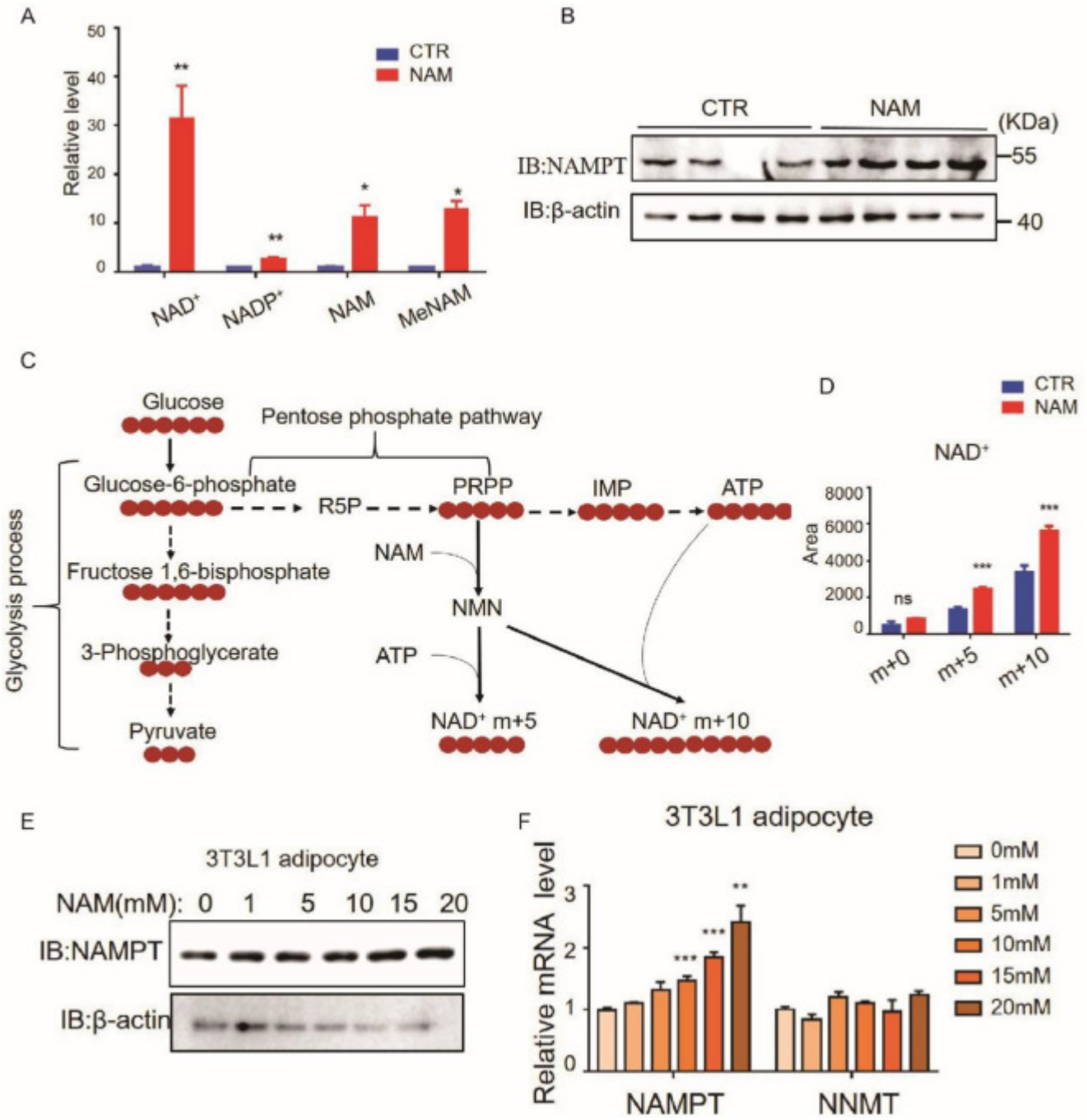

Download : Download high-res image (725KB) Download : Download full-size image

Fig. 2. NAM increased NAMPT and enhanced NAD+ biosynthesis (A). NAD^+, $NADP^+$, NAM, and N^1-methylnicotinamide (MeNAM), which were corrected with the tissue mass, were increased in adipose tissue by NAM supplementation. Data were presented as mean ± SD, $^*P < .05$, $^{**}P < .01$, $n = 4–6$ mice per group. (B) Representative image showed that NAM supplementation increased abundance of NAMPT in adipose tissue. (C) Graphic model showing stable isotopic tracing with $^{13}C_6$-glucose in 3T3L1 cells. Red blots represented ^{13}C labels of the intermediates. (D) The relative level of NAD^+ traced with $^{13}C_6$-glucose in 3T3L1 cells treated with or without NAM (10 mM). m + 0: zero carbon atom were labelled with ^{13}C, m + 5: five carbon atoms were labelled with ^{13}C, m +10: ten carbon atoms were labelled with ^{13}C. Data were presented as mean ± SD, ns: not

significant, ***$P < .001$, $n = 4$/ group. (E) Western blot showed that NAM supplementation increased abundance of NAMPT of 3T3L1 adipocytes. (F) mRNA level of NAMPT and NNMT of 3T3L1 adipocytes under NAM treatment at different dosages. Data were presented as mean ± SD. **$P < .01$ and ***$P < .001$, $n = 4$/ group. mRNA, messenger RNA; NAM, nicotinamide. (Color version of figure is available online.)

As shown in Figure 2C, glucose was consumed via glycolysis pathway to produce intermediate metabolites, such as F16BP, 3PG and pyruvate, or pentose phosphate pathway to produce 5-phosphoribosyl-1-pyrophosphate (PRPP). NAM treatment did not change the levels of F16P, and 3PG (Fig. S2D and E), suggesting glycolysis was not altered in NAM treated cells while PRPP was decreased (Fig. S2F). PRPP was used to synthesize NMN, which were converted into (m + 5) and (m + 10) NAD^+, in which 22% and 55% of NAD^+ were in (m + 5) and (m + 10) forms, respectively (Fig. 2C). NAM treatment increased the labelling efficiency in both (m + 5) and (m + 10) forms (Fig. 2D), suggesting that supplementary NAM enhanced NAD^+ biosynthesis. Moreover, in 3T3L1 cells, both protein level and messenger RNA (mRNA) level of NAMPT were increased while NNMT was not changed as the dosage of NAM increased (Fig. 2E and F). These data demonstrated that NAM increased NAMPT and enhance NAD^+ synthesis.

3.3. NAM treatment enhanced mitochondrial biogenesis and functions

To systematically examine the effects of NAM on adipose tissue, we performed quantitative proteomics of adipose tissues from untreated and NAM-treated mice, and we identified 4,716 proteins from adipose samples. Using the threshold of 1.3-fold change and P value <.05 from references [27,28], we identified 154 differentially expressed proteins (DEPs), in which 64 proteins were upregulated and 90 proteins were downregulated in NAM-treated adipose samples (Fig. 3A, Table S1). We performed ingenuity pathway analysis of these 154 DEPs to identify the biological pathways regulated by these DEPs. The results showed that NAM dramatically increased the abundance of proteins associated with oxidative phosphorylation (OXPHOS), fatty acid β-oxidation, TCA cycle and oxidative stress defense system (Fig. 3B). To confirm that mitochondrial proteins were upregulated, western blot analysis was used to examine the expressions of COXIV and SOD2 and found that NAM upregulated both proteins (Fig. 3C). Additionally, mRNA levels of mitochondrial genes, such as COXIV, COX8b, SOD1, SOD2, ACADm, and ACADl were increased (Fig. 3D). To confirm that NAM enhanced mitochondrial biogenesis, we performed quantitative polymerase chain reaction on PPARα and PGC1α and found that both genes were upregulated in NMN-treated mice (Fig. 3D).

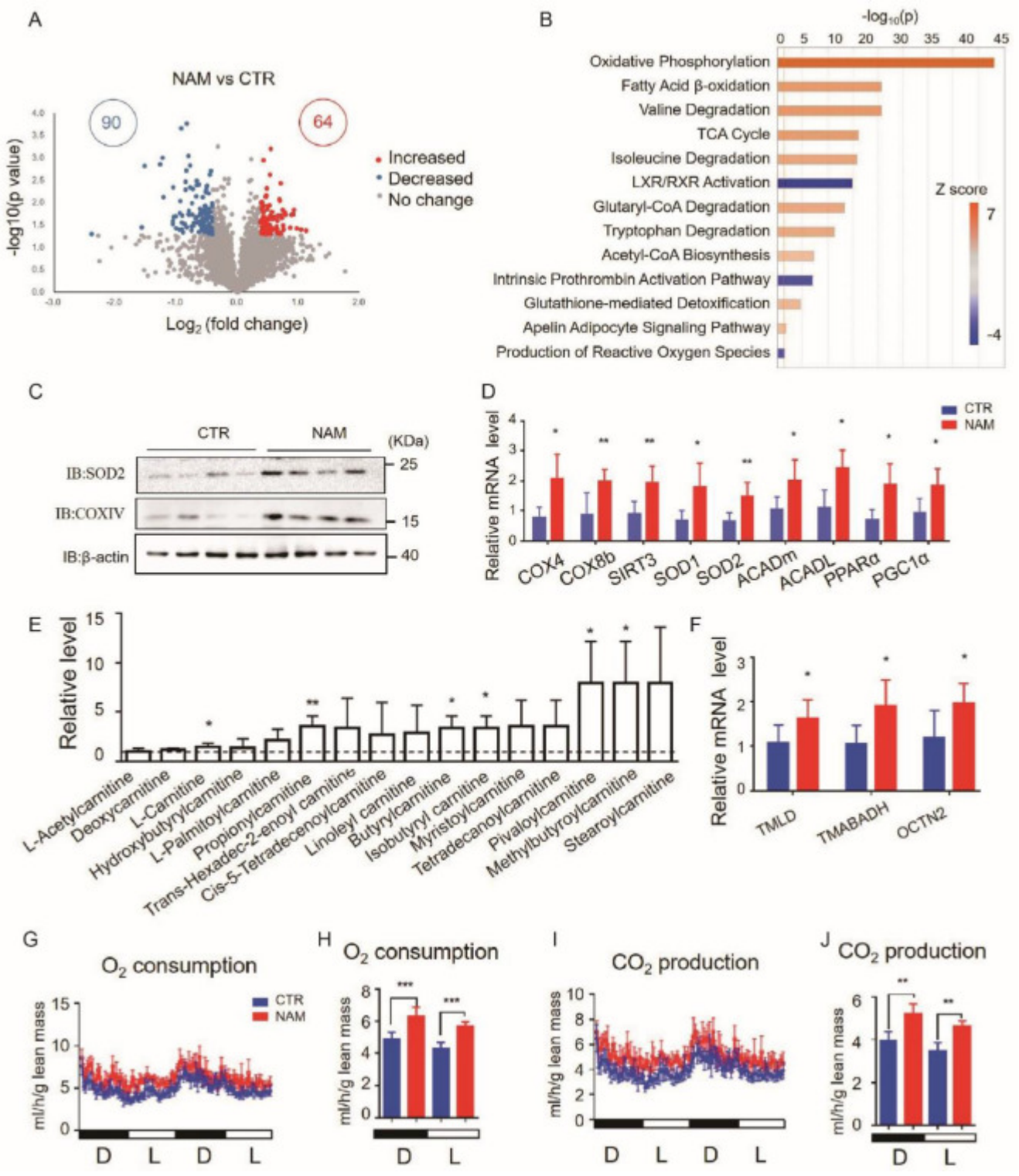

Download : Download high-res image (1MB) Download : Download full-size image

Fig. 3. NAM treatment enhanced mitochondrial biogenesis and functions (A) Volcano plot of proteome data from NAM treated SCAT *versus* control SCAT, red dots indicate the proteins with $P < .05$ and fold change > 1.3, green dots mean fold change <0.77 (1/1.3) and $P < .05$. (B) Significantly changed proteins (fold change < 0.76 or >1.30, $P < .05$) were uploaded to Ingenuity Pathway Analysis (IPA) software to perform pathway analysis. Red indicated activated pathways and blue

indicated downregulated pathways. (C) Immunoblot of SCAT using antibodies against SOD2, COXIV and β-actin. (D) mRNA level of SCAT treated with NAM or control. Data were presented as mean ± SD. $^{*}P < .05$ and $^{**}P < .01$, $n = 6$/ group. (E) NAM treatment increased carnitine level in SCAT relative to control group. Data were presented as mean ± SD, $^{*}P < .05$ and $^{**}P < .01$, $n = 6$/ group. (F) NAM increased SCAT mRNA level of carnitine synthesis gene. Data were presented as mean ± SD, $^{*}P < .05$, $n = 6$/ group. (G-J) NAM enhanced O_2 consumption (G, H) and CO_2 production (I, J) of mice, measured with metabolic cage and corrected with lean mass. Data were presented as mean ± SD. D: dark, L: light, $n = 4$/ group. NAM, nicotinamide. (Color version of figure is available online.)

It has been known that NAD^+, NAM, and N^1-methylnicotinamide mediate activity of SIRT1 and SIRT3 [29], [30], [31], and thus it is important to examine whether NAM supplementation alter the global protein acetylation. We analyzed the protein acetylation of adipose tissue and found that NAM globally decreased protein acetylation in adipose proteins (Fig. S3A). In particular, we identified that superoxide dismutase [Mn] (SOD2), a target of SIRT3, was less acetylated in NAM-treated adipose tissue (Fig. S3B), indicating that NAM enhanced activity of SIRT3, which was considered as a key regulator of mitochondrial biogenesis [32], [33], [34], [35]. To further explore how NAM enhanced mitochondrial functions, we examined the levels of adipose carnitines that are essential in fatty acid oxidation by importing fatty acids into mitochondria [[36], [37]], and found that acylcarnitine species were increased (Fig. 3E). Consistently, the gene expression levels of TMLD and TMABADH, which catalyze carnitine biosynthesis, were increased in NAM –treated adipose tissues (Fig. 3F). The expression of OCTN2, which encodes the transporter of free carnitine into cells from extracellular fluid, was also increased in NAM treated adipose tissue (Fig. 3F). Furthermore, NAM increased O_2 consumption and CO_2 production in DIO mice, which indicated the enhanced OXPHOS *in vivo* (Fig. 3G-J). These data confirmed that NAM improved mitochondrial biogenesis and functions in adipose tissue.

3.4. NAM increased glucose derived glutathione to maintain redox homeostasis

For GSH is important cellular antioxidant, we examined GSH and GSSG and found that NAM increased both GSH and GSSG in adipose tissue (Fig. 4A and B), which suggested that NAM increased the biosynthesis of glutathione. NAM meditated improvement of TCA provided abundant substrates for synthesis of glutathione. Accordingly, isotope-tracing assisted metabolic profiling revealed that about 67% of GSH and 90% of GSSG incorporated carbons from glucose (Fig. 4C). As intermediates for biosynthesis of GSH and GSSG, glutamate and glycine labeled from glucose were found to have distinct regulation by NAM treatment-increased abundance of glutamate but decreased abundance of glycine (Fig. 4D). Based on the labeling results in Figure 4D, enhanced biosynthesis of GSH and GSSG by NAM treatment was concluded through activating production of glutamate from glucose. Respectively, NAM increased the expression of GDH1, the enzyme linking the TCA and glutamate synthesis, both in 3T3L1 adipocytes and in

adipose tissue (Fig. 4E and F). These data suggested that NAM increased TCA-mediated glutathione synthesis.

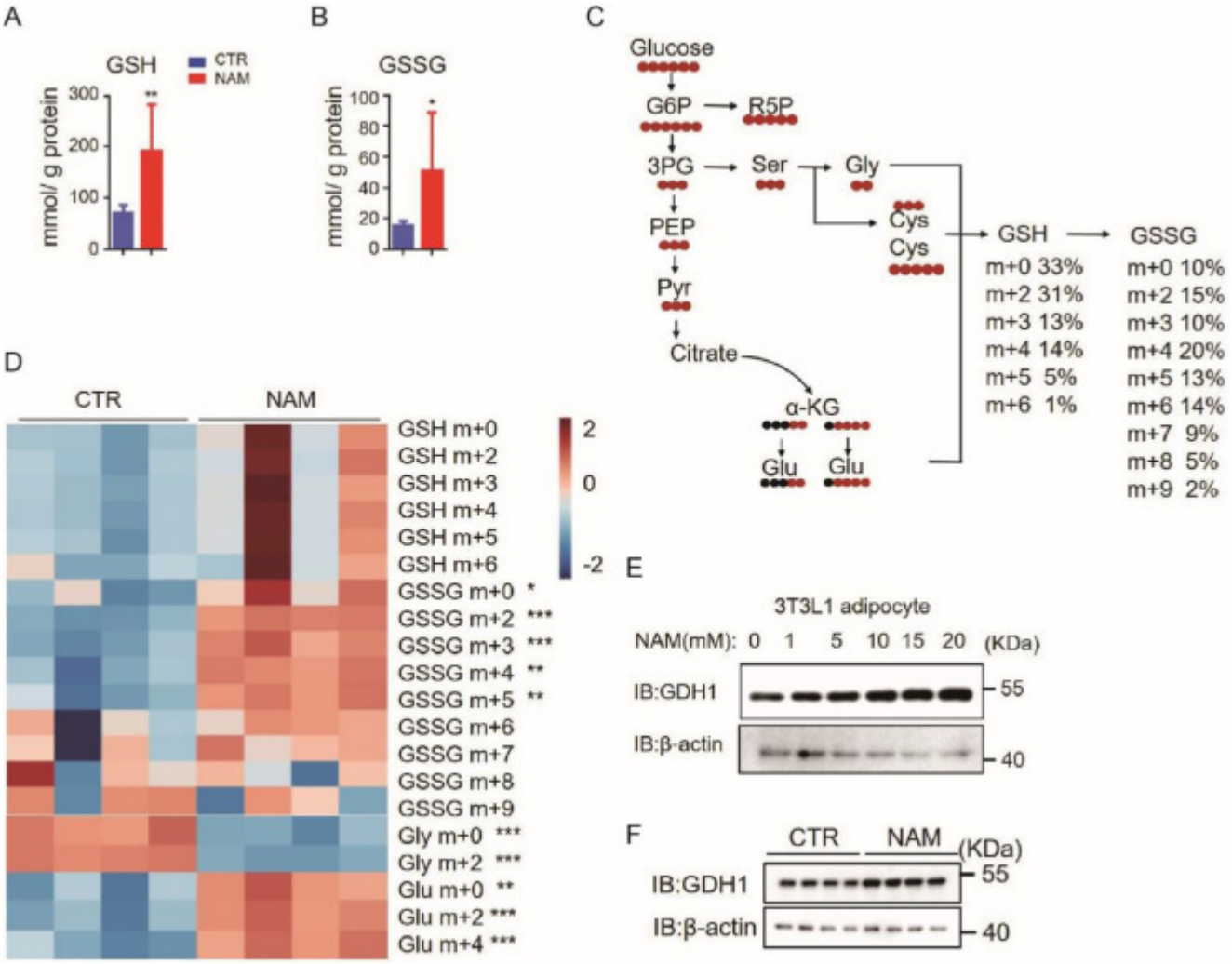

Download : Download high-res image (615KB)

Download : Download full-size image

Fig. 4. NAM increased glutathione biosynthesis (A, B) NAM supplementation increased adipose GSH and GSSG. Data were presented as mean ± Data were presented as mean ± SD. $^{*}P < .05$, $^{**}P < .01$, $n = 8$ mice per group. (C) Schematic picture showed the percentages of labelled GSH and GSSG traced with $^{13}C_6$-glucose in 3T3L1 control cells (without treatment of NAM). $N = 4$/ group. (D) Heat map demonstrated the relative changes of GSH, GSSG, glycine (Gly), and glutamate (Glu) in 3T3L1 cells treated with or without 10 mM NAM. $N = 4$/ group. (E) NAM increased protein level of glutamate dehydrogenase 1 (GDH1) in 3T3L1 adipocytes. Immunoblots shown were representative of three independent experiments. (F) NAM increased protein level of glutamate dehydrogenase 1 (GDH1) in SCAT. NAM, nicotinamide.

4. Discussion

Herein, we reported that NAM supplementation ameliorated metabolic dysfunction in high fat DIO mice. We found that NAM strikingly decreased mass of SCAT, and boosted adipose NAD^+, NADP, and N^1-methylNAM, in which NAD^+ was increased by 32-fold. The increase of lean mass partly contributed to the dramatic increase of NAD^+ level. Interestingly, NAM also upregulated NAMPT expression, the rate limiting enzyme in NAD^+ synthesis from NAM [38,39], and thus suggested that NAM reprogrammed NAD^+ salvage pathway. The elevated NAD^+ activated SIRTUINs. Consequently, protein acetylation was decreased in NAM-treated adipose tissue. Furthermore, the decreased acetylation intensity of SOD2 suggested that NAM improved the function of SIRT3, the major mitochondrial deacetylase to control mitochondrial biogenesis [33,35,40,41]. NAM-enhanced mitochondrial biogenesis was confirmed by proteomic analysis showing that mitochondrial proteins involved in fatty acid β oxidation, OXPHOS and TCA were all upregulated in adipose tissue. Consistently, NAM also increased O_2 consumption, CO_2 production, and adipose acylcarnitine levels by increasing expression of genes for carnitine biosynthesis in DIO mice. However, our study used four mice each group for metabolic cage measurement and six mice each group for metabolites quantitation, GTT and body composition analysis. Experiments using a larger pool of animals are needed to provided more quantifiable evidence.

On the other hand, mitochondria ROS, mainly from the complexes I and III of electron transport chain, are major source of cellular ROS [42], [43], [44]. Enhanced OXPHOS and oxidation of fatty acids alter the production of OXPHOS-associated ROS [45,46]. Excessive ROS can cause damages to DNA, lipids, and proteins [47]. GSH was increased by 3-old while GSSG was increased by 1.5-fold in NAM-treated adipose tissue, indicating biosynthesis of glutathione was enhanced to be able to defend against oxidative stress. TCA not only generates NADH for ATP production, but it also provides intermediate metabolites for glutathione synthesis. Isotopic tracing with $^{13}C_6$-glucose in adipocytes showed that NAM treatment increased glucose-derived glutathione, suggesting that NAM supplementation increased the SOD2 activity and GSH levels to eliminate excessive ROS.

This study has evaluated the function and mechanism of high-dose NAM on obesity and concluded that high-dose NAM ameliorated obesity after 2 weeks. In OLETF rats, 4-week supplementation of 100 mg NAM/kg BW/d increased NAD^+ and improved glucose metabolism [14]. However, in mice, 8-week supplementation of 100 mg NAM/kg BW/d induced glucose intolerance and skeletal muscle lipotoxicity [25]. Accordingly, in human, long-term intake of NAM was reported to result in depletion of S-adenosylmethionine and induce metabolic disorders [26,48,49]. NAM supplementation improved obesity efficiently and quickly. NAM did not change activities and food intakes of obese mice. NAM did not result in diarrhoea or vomiting. Blood AST, LDH, CK, creatinine, and uric acid were not increased, suggesting NAM did lead to injury of liver, heart, and kidney. Besides, for lean mice, blood proteins including AST, LDH, CK, and ALP were not increased by NAM supplementation, suggesting NAM supplementation did not cause injury in liver and heart for lean mice.

In conclusion, our results provided a systemic perspective of effects of NAM on adipose tissue by reprogramming metabolic pathway to enhance mitochondrial biogenesis, and increased GSH production. These results suggested that NAM supplementation was an effective approach to increase fatty acid catabolism and to ameliorate obesity.

Acknowledgments

We thank the Proteomics Facility and Metabolomics Core Facility at Technology Center of Protein Research at Tsinghua University for sample analysis.

Declaration of Competing Interest

The authors declare no competing interests.

Funding

This work was supported by Beijing Municipal Science and Technology Commission (No. 5214025), the Ministry of Science and Technology of the People's Republic of China (Grant No. 2017ZX10201101 and No. 2020YFC2002705), National Key Research and Development Program of China (Grant No. 2017YFA0505103).

CRediT authorship contribution statement

Chengting Luo: Investigation, Validation, Writing – original draft, Funding acquisition. **Changmei Yang:** Investigation, Validation. **Xueying Wang:** Investigation, Validation. **Yuling Chen:** Investigation. **Xiaohui Liu:** Validation, Writing – original draft, Supervision. **Haiteng Deng:** Funding acquisition, Writing – review & editing, Project administration, Supervision.

Appendix. Supplementary materials

Download all supplementary files Help

Download : **Download spreadsheet (19KB)**

Download : **Download Word document (961KB)**

Recommended articles

Reference

[1] A.V. Khera, M. Chaffin, K.H. Wade, S. Zahid, J. Brancale, R. Xia, M. Distefano, O. Senol-Cosar, M.E. Haas, A. Bick, *et al.*
Polygenic Prediction of Weight and Obesity Trajectories from Birth to Adulthood
Cell, 177 (2019), pp. 587-596.e589
View Record in Scopus Google Scholar

[2] J. Yoshino, Kathryn F. Mills, Myeong J. Yoon, S.-i. Imai
Nicotinamide Mononucleotide, a Key NAD+ Intermediate, Treats the Pathophysiology of Diet- and Age-Induced Diabetes in Mice
Cell Metabolism, 14 (2011), pp. 528-536
Article Download PDF View Record in Scopus Google Scholar

[3] S.A. Trammell, B.J. Weidemann, A. Chadda, M.S. Yorek, A. Holmes, L.J. Coppey, A. Obrosov, R.H. Kardon, M.A. Yorek, C. Brenner
Nicotinamide Riboside Opposes Type 2 Diabetes and Neuropathy in Mice
Scientific reports, 6 (2016), p. 26933
View Record in Scopus Google Scholar

[4] David W. Frederick, E. Loro, L. Liu, A. Davila, K. Chellappa, Ian M. Silverman, William J. Quinn, Sager J. Gosai, Elisia D. Tichy, James G. Davis, *et al.*
Loss of NAD Homeostasis Leads to Progressive and Reversible Degeneration of Skeletal Muscle
Cell Metabolism, 24 (2016), pp. 269-282
Article Download PDF View Record in Scopus Google Scholar

[5] K. Gariani, K.J. Menzies, D. Ryu, C.J. Wegner, X. Wang, E.R. Ropelle, N. Moullan, H. Zhang, A. Perino, V. Lemos, *et al.*
Eliciting the mitochondrial unfolded protein response by nicotinamide adenine dinucleotide repletion reverses fatty liver disease in mice
Hepatology (Baltimore, Md.), 63 (2016), pp. 1190-1204
CrossRef View Record in Scopus Google Scholar

[6] K.A. Hershberger, A.S. Martin, M.D. Hirschey
Role of NAD+ and mitochondrial sirtuins in cardiac and renal diseases
Nature Reviews Nephrology, 13 (2017), p. 213
CrossRef View Record in Scopus Google Scholar

[7] H. Yang, T. Yang, J.A. Baur, E. Perez, T. Matsui, J.J. Carmona, D.W. Lamming, N.C. Souza-Pinto, V.A. Bohr, A. Rosenzweig, *et al.*
Nutrient-sensitive mitochondrial NAD+ levels dictate cell survival
Cell, 130 (2007), pp. 1095-1107
Article Download PDF View Record in Scopus Google Scholar

[8] E. Roh, G. Myoung Kang, S. Young Gil, C. Hee Lee, S. Kim, D. Hong, G. Hoon Son, M.S. Kim
Effects of Chronic NAD Supplementation on Energy Metabolism and Diurnal Rhythm in Obese Mice
Obesity (Silver Spring, Md.), 26 (2018), pp. 1448-1456
CrossRef View Record in Scopus Google Scholar

[9] C. Canto, K.J. Menzies, J. Auwerx
NAD(+) Metabolism and the Control of Energy Homeostasis: A Balancing Act between Mitochondria and the Nucleus
Cell Metab, 22 (2015), pp. 31-53
Article Download PDF View Record in Scopus Google Scholar

[10] L. Liu, X. Su, W.J. Quinn 3rd, S. Hui, K. Krukenberg, D.W. Frederick, P. Redpath, L. Zhan, K. Chellappa, E. White, *et al.*
Quantitative Analysis of NAD Synthesis-Breakdown Fluxes
Cell Metab, 27 (2018), pp. 1067-1080
Google Scholar

[11] J. Yoshino, J.A. Baur, S.I. Imai
NAD(+) Intermediates: The Biology and Therapeutic Potential of NMN and NR
Cell Metab, 27 (2018), pp. 513-528
Article Download PDF View Record in Scopus Google Scholar

[12] D. Fangmann, E.M. Theismann, K. Turk, D.M. Schulte, I. Relling, K. Hartmann, J.K. Keppler, J.R. Knipp, A. Rehman, F.A. Heinsen, *et al.*
Targeted Microbiome Intervention by Microencapsulated Delayed-Release Niacin Beneficially Affects Insulin Sensitivity in Humans
Diabetes Care, 41 (2018), pp. 398-405
CrossRef View Record in Scopus Google Scholar

[13] F.Q. Alenzi
Effect of nicotinamide on experimental induced diabetes
Iranian journal of allergy, asthma, and immunology, 8 (2009), pp. 11-18
View Record in Scopus Google Scholar

[14] C.M. John, R. Ramasamy, G.A. Naqeeb, A.H.D. Al-Nuaimi, A. Adam
Nicotinamide Supplementation Protects Gestational Diabetic Rats by Reducing Oxidative Stress and Enhancing Immune Responses
Current Medicinal Chemistry, 19 (2012), pp. 5181-5186
CrossRef View Record in Scopus Google Scholar

[15] S.J. Yang, J.M. Choi, L. Kim, S.E. Park, E.J. Rhee, W.Y. Lee, K.W. Oh, S.W. Park, C.Y. Park

Nicotinamide improves glucose metabolism and affects the hepatic NAD-sirtuin pathway in a rodent model of obesity and type 2 diabetes
J Nutr Biochem, 25 (2014), pp. 66-72
Article Download PDF Google Scholar

[16] C. Shen, X. Dou, Y. Ma, W. Ma, S. Li, Z. Song
Nicotinamide protects hepatocytes against palmitate-induced lipotoxicity via SIRT1-dependent autophagy induction
Nutrition Research, 40 (2017), pp. 40-47
Article Download PDF View Record in Scopus Google Scholar

[17] S.J. Mitchell, M. Bernier, M.A. Aon, S. Cortassa, E.Y. Kim, E.F. Fang, H.H. Palacios, A. Ali, I. Navas-Enamorado, A. Di Francesco, *et al.*
Nicotinamide Improves Aspects of Healthspan, but Not Lifespan, in Mice
Cell Metab, 27 (2018), pp. 667-676.e664
View Record in Scopus Google Scholar

[18] L. Ye, Z. Cao, X. Lai, Y. Shi, N. Zhou
Niacin Ameliorates Hepatic Steatosis by Inhibiting De Novo Lipogenesis Via a GPR109A-Mediated PKC-ERK1/2-AMPK Signaling Pathway in C57BL/6 Mice Fed a High-Fat Diet
J Nutr, 150 (2020), pp. 672-684
CrossRef View Record in Scopus Google Scholar

[19] A. Couturier, R. Ringseis, E. Most, K. Eder
Pharmacological doses of niacin stimulate the expression of genes involved in carnitine uptake and biosynthesis and improve the carnitine status of obese Zucker rats
BMC Pharmacology and Toxicology, 15 (2014), p. 37
View Record in Scopus Google Scholar

[20] L. Jin, Y. Huo, Z. Zheng, X. Jiang, H. Deng, Y. Chen, Q. Lian, R. Ge, H. Deng
Down-regulation of Ras-related protein Rab 5C-dependent endocytosis and glycolysis in cisplatin-resistant ovarian cancer cell lines
Mol Cell Proteomics, 13 (2014), pp. 3138-3151
Article Download PDF CrossRef View Record in Scopus Google Scholar

[21] M. Yuan, S.B. Breitkopf, X. Yang, J.M. Asara
A positive/negative ion-switching, targeted mass spectrometry-based metabolomics platform for bodily fluids, cells, and fresh and fixed tissue
Nature protocols, 7 (2012), pp. 872-881
CrossRef View Record in Scopus Google Scholar

[22] H. Tang, R. Teng, X. Zhao, X. Wang, L. Xu, H. Deng, X. Liu

Isotope tracing assisted metabolic profiling: Application to understanding HSP60 silencing mediated tumor progression
Analytica chimica acta, 1047 (2019), pp. 93-103
Article Download PDF View Record in Scopus Google Scholar

[23] J. Guo, X. Li, W. Zhang, Y. Chen, S. Zhu, L. Chen, R. Xu, Y. Lv, D. Wu, M. Guo, *et al.*
HSP60-regulated Mitochondrial Proteostasis and Protein Translation Promote Tumor Growth of Ovarian Cancer
Scientific reports, 9 (2019), p. 12628
View Record in Scopus Google Scholar

[24] Y. Perez-Riverol, A. Csordas, J. Bai, M. Bernal-Llinares, S. Hewapathirana, D.J. Kundu, A. Inuganti, J. Griss, G. Mayer, M. Eisenacher, *et al.*
The PRIDE database and related tools and resources in 2019: improving support for quantification data
Nucleic Acids Res, 47 (2019), pp. D442-D450
CrossRef View Record in Scopus Google Scholar

[25] Z. Qi, J. Xia, X. Xue, Q. He, L. Ji, S. Ding
Long-term treatment with nicotinamide induces glucose intolerance and skeletal muscle lipotoxicity in normal chow-fed mice: compared to diet-induced obesity
The Journal of Nutritional Biochemistry, 36 (2016), pp. 31-41
Article Download PDF View Record in Scopus Google Scholar

[26] S.S. Zhou, D. Li, W.P. Sun, M. Guo, Y.Z. Lun, Y.M. Zhou, F.C. Xiao, L.X. Jing, S.X. Sun, L.B. Zhang, *et al.*
Nicotinamide overload may play a role in the development of type 2 diabetes
World journal of gastroenterology, 15 (2009), pp. 5674-5684
CrossRef View Record in Scopus Google Scholar

[27] C.S. Gan, P.K. Chong, T.K. Pham, P.C. Wright
Technical, experimental, and biological variations in isobaric tags for relative and absolute quantitation (iTRAQ)
J Proteome Res, 6 (2007), pp. 821-827
CrossRef Google Scholar

[28] T. Suriyanarayanan, L. Qingsong, L.T. Kwang, L.Y. Mun, T. Truong, C.J. Seneviratne
Quantitative Proteomics of Strong and Weak Biofilm Formers of Enterococcus faecalis Reveals Novel Regulators of Biofilm Formation
Mol Cell Proteomics, 17 (2018), pp. 643-654
Article Download PDF CrossRef View Record in Scopus Google Scholar

[29]

S. Hong, J.M. Moreno-Navarrete, X. Wei, Y. Kikukawa, I. Tzameli, D. Prasad, Y. Lee, J.M. Asara, J.M. Fernandez-Real, E. Maratos-Flier, *et al.*
Nicotinamide N-methyltransferase regulates hepatic nutrient metabolism through Sirt1 protein stabilization
Nat Med, 21 (2015), pp. 887-894
CrossRef View Record in Scopus Google Scholar

[30] E.S. Hwang, S.B. Song
Nicotinamide is an inhibitor of SIRT1 in vitro, but can be a stimulator in cells
Cellular and Molecular Life Sciences, 74 (2017), pp. 3347-3362
CrossRef View Record in Scopus Google Scholar

[31] S.-y. Jang, H.T. Kang, E.S. Hwang
Nicotinamide-induced Mitophagy: EVENT MEDIATED BY HIGH NAD+/NADH RATIO AND SIRT1 PROTEIN ACTIVATION
Journal of Biological Chemistry, 287 (2012), pp. 19304-19314
Article Download PDF CrossRef View Record in Scopus Google Scholar

[32] A.S. Hebert, K.E. Dittenhafer-Reed, W. Yu, D.J. Bailey, E.S. Selen, M.D. Boersma, J.J. Carson, M. Tonelli, A.J. Balloon, A.J. Higbee, *et al.*
Calorie restriction and SIRT3 trigger global reprogramming of the mitochondrial protein acetylome
Mol Cell, 49 (2013), pp. 186-199
Article Download PDF View Record in Scopus Google Scholar

[33] M.D. Hirschey, T. Shimazu, E. Jing, C.A. Grueter, A.M. Collins, B. Aouizerat, A. Stancakova, E. Goetzman, M.M. Lam, B. Schwer, *et al.*
SIRT3 deficiency and mitochondrial protein hyperacetylation accelerate the development of the metabolic syndrome
Mol Cell, 44 (2011), pp. 177-190
Article Download PDF View Record in Scopus Google Scholar

[34] A.A. Kendrick, M. Choudhury, S.M. Rahman, C.E. McCurdy, M. Friederich, J.L. Van Hove, P.A. Watson, N. Birdsey, J. Bao, D. Gius, *et al.*
Fatty liver is associated with reduced SIRT3 activity and mitochondrial protein hyperacetylation
Biochem J, 433 (2011), pp. 505-514
View Record in Scopus Google Scholar

[35] H. Liu, S. Li, X. Liu, Y. Chen, H. Deng
SIRT3 Overexpression Inhibits Growth of Kidney Tumor Cells and Enhances Mitochondrial Biogenesis

J Proteome Res, 17 (2018), p. 10
Article Download PDF CrossRef Google Scholar

[36] C.J. Rebouche, H. Seim
Carnitine metabolism and its regulation in microorganisms and mammals
Annual review of nutrition, 18 (1998), pp. 39-61
CrossRef View Record in Scopus Google Scholar

[37] F.M. Vaz, R.J. Wanders
Carnitine biosynthesis in mammals
Biochem J, 361 (2002), pp. 417-429
View Record in Scopus Google Scholar

[38] J.R. Revollo, A.A. Grimm, S. Imai
The NAD biosynthesis pathway mediated by nicotinamide phosphoribosyltransferase regulates Sir2 activity in mammalian cells
J Biol Chem, 279 (2004), pp. 50754-50763
Article Download PDF View Record in Scopus Google Scholar

[39] M. Yoshida, A. Satoh, J.B. Lin, K.F. Mills, Y. Sasaki, N. Rensing, M. Wong, R.S. Apte, S.I. Imai
Extracellular Vesicle-Contained eNAMPT Delays Aging and Extends Lifespan in Mice
Cell Metab, 30 (2019), pp. 329-342.e325
View Record in Scopus Google Scholar

[40] A. Tyagi, C.U. Nguyen, T. Chong, C.R. Michel, K.S. Fritz, N. Reisdorph, L. Knaub, J.E.B. Reusch, S. Pugazhenthi
SIRT3 deficiency-induced mitochondrial dysfunction and inflammasome formation in the brain
Scientific reports, 8 (2018), p. 17547
View Record in Scopus Google Scholar

[41] Q. Wang, L. Li, C.Y. Li, Z. Pei, M. Zhou, N. Li
SIRT3 protects cells from hypoxia via PGC-1alpha- and MnSOD-dependent pathways
Neuroscience, 286 (2015), pp. 109-121
Article Download PDF Google Scholar

[42] M.P. Murphy
How mitochondria produce reactive oxygen species
Biochem J, 417 (2009), pp. 1-13
Google Scholar

[43]

M.A. Siddiqui, J. Ahmad, N.N. Farshori, Q. Saquib, S. Jahan, M.P. Kashyap, M. Ahamed, J. Musarrat, A.A. Al-Khedhairy
Rotenone-induced oxidative stress and apoptosis in human liver HepG2 cells
Mol Cell Biochem, 384 (2013), pp. 59-69
CrossRef View Record in Scopus Google Scholar

[44] R. Stefanatos, A. Sanz
The role of mitochondrial ROS in the aging brain
FEBS Lett, 592 (2018), pp. 743-758
CrossRef View Record in Scopus Google Scholar

[45] J.M. Weiss, L.C. Davies, M. Karwan, L. Ileva, M.K. Ozaki, R.Y. Cheng, L.A. Ridnour, C.M. Annunziata, D.A. Wink, D.W. McVicar
Itaconic acid mediates crosstalk between macrophage metabolism and peritoneal tumors
J Clin Invest, 128 (2018), pp. 3794-3805
CrossRef View Record in Scopus Google Scholar

[46] G.S. Shadel, T.L. Horvath
Mitochondrial ROS signaling in organismal homeostasis
Cell, 163 (2015), pp. 560-569
Article Download PDF View Record in Scopus Google Scholar

[47] M. Chattopadhyay, V.K. Khemka, G. Chatterjee, A. Ganguly, S. Mukhopadhyay, S. Chakrabarti
Enhanced ROS production and oxidative damage in subcutaneous white adipose tissue mitochondria in obese and type 2 diabetes subjects
Molecular and Cellular Biochemistry, 399 (2015), pp. 95-103
CrossRef View Record in Scopus Google Scholar

[48] M. Liu, L. Li, J. Chu, B. Zhu, Q. Zhang, X. Yin, W. Jiang, G. Dai, W. Ju, Z. Wang, *et al.*
Serum N(1)-Methylnicotinamide Is Associated With Obesity and Diabetes in Chinese
J Clin Endocrinol Metab, 100 (2015), pp. 3112-3117
CrossRef View Record in Scopus Google Scholar

[49] S.-S. Zhou, D. Li, Y.-M. Zhou, W.-P. Sun, Q.-G. Liu
B-vitamin consumption and the prevalence of diabetes and obesity among the US adults: population based ecological study
BMC Public Health, 10 (2010), p. 746
View Record in Scopus Google Scholar

Cited by (0)